

# Structural and Reactivity Studies of a Cyanoacetic Acid Derivative of Tungsten Pentacarbonyl. X-ray Structure of $W(CO)_5NCCH_2COOH$

Donald J. Darensbourg,\* Earl V. Atnip, and Joseph H. Reibenspies

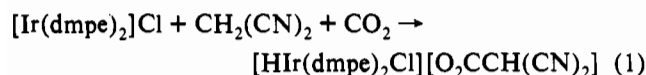
Department of Chemistry, Texas A&M University, College Station, Texas 77843

Received March 5, 1992

The new cyanoacetic acid complex  $W(CO)_5NCCH_2COOH$  (**1**) has been synthesized from the reaction of  $W(CO)_5THF$  and  $NCCH_2COOH$ . The molecular structure of **1** has been determined by X-ray diffraction methods. The compound crystallizes in the triclinic space group  $P\bar{1}$  with two molecules in a cell of dimensions  $a = 6.7390$  (10) Å,  $b = 9.745$  (2) Å,  $c = 10.241$  (2) Å,  $\alpha = 63.57$  (2)°,  $\beta = 81.71$  (2)°,  $\gamma = 76.22$  (2)°. Full-matrix least-squares refinement gives final  $R$  and  $R_w$  on  $F$  of 0.026 and 0.037 for 2030 observed [ $F > 4\sigma(F)$ ] data. The structure confirms the presence of the nitrile ligand located 2.178 (7) Å from the tungsten center, with the carboxyl groups of two molecules coupled by strong intermolecular hydrogen-bonding ( $O-H\cdots O = 2.627$  (3) Å). This hydrogen-bonding structure was observed as well in solution as indicated by infrared spectroscopy. The displacement of the cyanoacetic acid ligand in **1** by carbon monoxide was shown to proceed via a solvent-assisted  $I_d$  process in tetrahydrofuran and by a  $D$  process in the less-interacting solvent methylene chloride. The activation parameters for these processes are consistent with the proposed mechanism, with  $\Delta H^\ddagger$  and  $\Delta S^\ddagger$  for the displacement of the  $NCCH_2COOH$  ligand determined to be 19.4 kcal/mol and  $-14.7$  eu in THF and 29.2 kcal/mol and 11.8 eu in  $CH_2Cl_2$ , respectively. Comparable kinetic data were observed for the tungsten complexes containing the electronically similar ligands  $NC(CH_2)_{10}COOH$  and  $CH_3CN$ . The relevance of this study to the catalytic decarboxylation reaction of cyanoacetic acid in the presence of  $W(CO)_5O_2CCH_2CN^-$  is discussed.

## Introduction

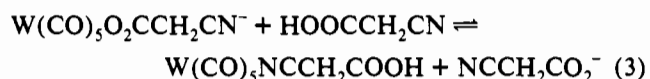
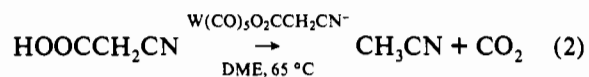
There have been reports of the activation of acidic C-H bonds by electron-rich complexes of iridium(I) and rhodium(I) in the presence of carbon dioxide to provide the corresponding protonated metal cationic complex and carboxylate anion.<sup>1-4</sup> For example,  $[Ir(dmpe)_2]Cl$  reacts with malonodinitrile and  $CO_2$  according to eq 1 to provide the protonated complex and the dicyanoacetate



anion.<sup>1,2</sup> A similar reaction between  $[Ir(depe)_2]Cl$  and  $CH_3CN$  has been described by English and Herskovitz.<sup>3</sup>

In an effort to gain more mechanistic insight into these processes we have been investigating the reverse reaction, i.e., the catalytic decarboxylation of cyanoacetic acid to yield acetonitrile and carbon dioxide. Furthermore, in order to assess the generality of such reactions, a question of particular concern to us was the role of the cyano substituent in these processes.<sup>5</sup> With regard to this question we have been examining the binding of carboxylic acids which contain cyano substituents to transition metals. Previously, results of cyanoacetic acid bound to Cu(I) via the nitrile group have been presented.<sup>6</sup> Herein, we wish to present the X-ray crystal structure of  $W(CO)_5(NCCH_2COOH)$  (**1**) along with a kinetic investigation for the displacement of various nitriles from tungsten pentacarbonyl. The choice of this particular derivative is governed by the fact that  $W(CO)_5O_2CCH_2CN^-$  is an effective catalyst precursor for the decarboxylation of

cyanoacetic acid (eq 2), and that this catalytic process is inhibited by the formation of **1** according to eq 3.<sup>5,7</sup>



## Experimental Section

**Methods and Materials.** All manipulations were performed on a double-manifold Schlenk vacuum line under an atmosphere of argon or in an argon-filled glovebox. Solvents were dried and deoxygenated by distillation from the appropriate reagent under a nitrogen atmosphere. Photolysis experiments were performed using a mercury arc 450-W UV immersion lamp purchased from Ace Glass Co. Infrared spectra were recorded on a Mattson 6020 spectrometer with DTGS and MCT detectors. Routine infrared spectra were collected using a 0.10-mm  $CaF_2$  cell. Kinetic measurements were made using a CIRCLE (cylindrical internal reflectance) cell furnished by Spectra Tech Inc. The temperature was held to within 1 °C by a Parr temperature controller and was monitored by an Omega thermocouple.  $^1H$  and  $^{13}C$  NMR spectra were obtained on a Varian XL-200 spectrometer.  $W(CO)_6$  was purchased from Strem Chemicals, Inc., and used without further purification.  $NCCH_2COOH$  and  $NC(CH_2)_{10}COOH$  were purchased from Aldrich Chemical Co., and were dried in a vacuum oven at 40 °C prior to use. Microanalyses and molecular weight determination were performed by Galbraith Laboratories, Inc., Knoxville, TN.

**Syntheses of  $W(CO)_5(NC-R)$  Derivatives.** The synthesis  $W(CO)_5(NC-R)$  was accomplished in > 90% yield by the reaction of  $W(CO)_5THF$  with 1 equiv of  $NC-R$  at ambient temperature, where  $R = -CH_2COOH$ ,  $-(CH_2)_{10}COOH$ , and  $-CH_3$ . The THF was removed from the reaction mixture by vacuum and the remaining light yellow-green solid was washed with hexane three times to afford a light green powder. Anal. Calcd for  $W(CO)_5NCCH_2COOH$  ( $C_8H_7NO_7W$ ): C, 23.50; H, 0.739. Found: C, 23.42; H, 0.85. Molecular weight determined by vapor phase osmom-

- Behr, A.; Herdtweck, E.; Herrmann, W. A.; Keim, W.; Kipshagen, W. *Organometallics* **1987**, *6*, 2307.
- Behr, A. *Carbon Dioxide Activation by Metal Complexes*; VCH Publishing: Weinheim, Germany, 1988.
- English, A. D.; Herskovitz, T. *J. Am. Chem. Soc.* **1977**, *99*, 1648.
- Ittel, S. D.; Tolman, C. A.; English, A. D.; Jesson, J. P. *J. Am. Chem. Soc.* **1978**, *100*, 7577.
- Darensbourg, D. J.; Joyce, J. A.; Rheingold, A. *Organometallics* **1991**, *10*, 3407.
- Darensbourg, D. J.; Longridge, E. M.; Atnip, E. V.; Reibenspies, J. H. *Inorg. Chem.* **1991**, *30*, 358.

- Chojnacki, J. A.; Darensbourg, D. J. Presented at the Fourth Chemical Congress of North America, New York, NY, August, 1991; Paper INOR 212.



Table III. Crystallographic Data and Data Collection Parameters for 1

formula	C <sub>8</sub> H <sub>3</sub> NO <sub>7</sub> W	calcd density ρ, gm/cm <sup>3</sup>	2.324
habit	needle	crystal size, mm	0.22 × 0.25 × 1.5
fw	409	abs coeff μ, cm <sup>-1</sup>	101.17
space	triclinic P $\bar{1}$	scan type	ω
a, Å	6.7390 (10)	2θ range	4.0–50.0
b, Å	9.745 (2)	no. of unique reflns	2030
c, Å	10.241 (2)	no. of observed reflns	2030 (F > 4.0σ(F))
α, deg	63.57 (2)	data-param ratio	13.1:1
β, deg	81.71 (2)	final residuals (obsd data) <sup>a</sup>	R = 2.64%; R <sub>w</sub> = 3.68%
γ, deg	76.22 (2)	residuals (all data)	R = 2.64%; R <sub>w</sub> = 3.68%
V, Å <sup>3</sup>	584.4 (2)	goodness of fit	S = 5.30
molecules/cell	2		

$$^a R = \sum |F_o - F_c| / \sum F_o. R_w = \{[\sum w(F_o - F_c)^2] / [\sum w(F_o)^2]\}^{1/2}. S = \{[\sum w(F_o - F_c)^2] / [N_{data} - N_{param}]\}^{1/2}.$$

Table IV. Atomic Coordinates (×10<sup>4</sup>) and Equivalent Isotropic Displacement Parameters (Å<sup>2</sup> × 10<sup>3</sup>) for 1

	x	y	z	U(eq) <sup>a</sup>
W1	2621 (1)	2865 (1)	7895 (1)	22 (1)
C1	2025 (11)	674 (9)	8631 (8)	30 (3)
O1	1718 (9)	-541 (6)	8959 (7)	47 (3)
C2	3223 (11)	5064 (9)	6998 (8)	32 (3)
O3	3579 (10)	6290 (6)	6412 (7)	56 (3)
C3	-399 (12)	3707 (9)	8303 (8)	34 (3)
O3	-2044 (9)	4202 (7)	8544 (7)	53 (3)
C4	-5628 (11)	2075 (8)	7509 (8)	31 (3)
O4	7279 (9)	1633 (8)	7231 (7)	53 (3)
C5	1896 (12)	3268 (8)	5930 (8)	31 (3)
O5	1485 (10)	3512 (6)	4789 (6)	48 (3)
N1	3310 (9)	2424 (7)	10078 (7)	31 (3)
C6	3547 (11)	2147 (8)	11261 (8)	29 (3)
C7	3817 (10)	1729 (8)	12800 (7)	31 (3)
C8	2111 (10)	981 (7)	13789 (7)	26 (3)
O6	347 (7)	1457 (6)	13172 (5)	35 (2)
O7	2423 (7)	50 (6)	15050 (5)	34 (2)

<sup>a</sup> Equivalent isotropic U defined as one-third of the trace of the orthogonalized U<sub>ij</sub> tensor.

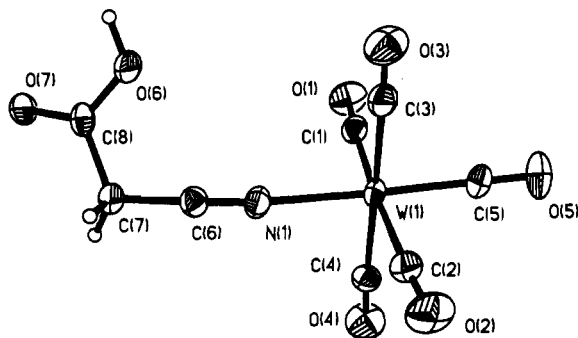


Figure 2. ORTEP plot of 1 with the atom-numbering scheme. Thermal ellipsoids enclose 50% of the electron density.

the dimer is held together via intermolecular hydrogen-bonding. On the other hand, in tetrahydrofuran solution both the metal-complexed and uncomplexed monomeric acid are hydrogen-bonded to THF (i.e., as depicted in species A). Further evidence for this is seen when a small amount of THF (5% by volume) is added to a solution of 1 in CH<sub>2</sub>Cl<sub>2</sub>, where the ν(C=O) region of the infrared spectrum is identical to what is observed in pure THF.

**Solid-State Structure of W(CO)<sub>5</sub>NCCH<sub>2</sub>COOH (1).** Crystallographic data and data collection parameters for 1 determined at 193 K may be found in Table III. Final atomic coordinates for all non-hydrogen atoms are provided in Table IV. An ORTEP view of 1 is shown in Figure 2 along with the atom-numbering scheme. The pertinent bond distances and bond angles are listed in Tables V and VI, respectively. The anisotropic thermal parameters for all non-hydrogen atoms and the calculated atomic coordinates for the hydrogen atoms in crystalline W(CO)<sub>5</sub>(NCCH<sub>2</sub>COOH) are available as supplementary material.

The carboxylic acid complex 1 exists as a slightly distorted

Table V. Selected Bond Lengths (Å) for 1

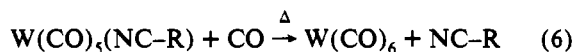
W1-C1	2.044 (8)	W1-C2	2.039 (8)
W1-C2	2.063 (8)	W1-C4	2.038 (7)
W1-C5	1.982 (9)	W1-N1	2.178 (7)
C1-O1	1.14 (1)	C2-O2	1.14 (1)
C3-O3	1.14 (1)	C4-O4	1.138 (9)
C5-O5	1.15 (1)	N1-C6	1.15 (1)
C6-C7	1.47 (1)	C7-C8	1.512 (9)
C8-O6	1.311 (9)	C8-O7	1.217 (7)

Table VI. Selected Bond Angles (deg) for 1

C1-W1-C2	175.5 (4)	C1-W1-C3	90.4 (3)
C2-W1-C3	90.7 (3)	C1-W1-C4	90.9 (3)
C2-W1-C4	88.0 (3)	C3-W1-C4	178.4 (4)
C1-W1-C5	87.8 (3)	C2-W1-C5	87.9 (3)
C3-W1-C5	88.8 (3)	C4-W1-C5	92.2 (3)
C1-W1-N1	91.6 (3)	C2-W1-N1	92.8 (3)
C3-W1-N1	89.5 (3)	C4-W1-N1	89.6 (3)
C5-W1-N1	178.1 (3)	W1-C1-O1	175.9 (7)
W1-C2-O2	175.7 (8)	W1-C3-O3	178.0 (1)
W1-C4-O4	176.5 (8)	W1-C5-O5	179.4 (8)
W1-N1-C6	175.0 (6)	N1-C6-C7	177.5 (8)
C6-C7-C8	112.0 (7)	C7-C8-O6	114.3 (5)
C7-C8-O7	120.3 (6)	O6-C8-O7	125.4 (6)

octahedron. The carboxylic acid ligand, bound to the tungsten center via the nitrile group, exhibits a significant trans influence similar to that seen in its oxygen bound carboxylate counterpart.<sup>9</sup> That is, the average W-C bond distance for the carbonyl ligands cis to the carboxylic acid ligand is notably longer at 2.043 [8] Å vs the trans at 1.982 (9) Å. The average C (trans)-W-C (cis) bond angle is 89.2 [3]°. The W-N bond distance is 2.178 (7) Å with a nearly linear W-N-C bond angle of 175.0 (6)°. This metal-nitrogen distance is quite similar to that observed for the analogous bond in the acetonitrile complex, *fac*-W(CO)<sub>3</sub>(CH<sub>3</sub>CN)(dppm), where a value of 2.190 (5) Å was observed.<sup>10</sup> The plane containing the acid function (-COOH) of cyanoacetic acid in complex 1 is tilted towards the C(3)-O cis carbonyl group forming an angle of 62.9° with the plane of cis CO ligands. Nevertheless, the closest carboxylic acid oxygen atom (O(6)-H) to the tungsten center is 4.516 Å. Complex 1 also exhibits strong intermolecular hydrogen bonding between the carboxylic functionalities (Figure 3).

**Kinetic Data for Ligand Substitution.** The nitrile ligands in W(CO)<sub>5</sub>(NC-R) derivatives are readily replaced by carbon monoxide according to eq 6. The kinetic parameters for reaction



6 were determined as a function of temperature over a range of 26 °C in THF, and these data are presented in Table VII. This process was observed to be first order in metal substrate and zero order in carbon monoxide at high CO pressures i.e., where [CO]

- (9) Darensbourg, D. J.; Joyce, J. A.; Bischoff, C. J.; Reibenspies, J. H. *Inorg. Chem.* 1991, 30, 1137.  
 (10) Darensbourg, D. J.; Zalewski, D. J.; Plepys, C.; Campana, C. *Inorg. Chem.* 1987, 26, 3727.

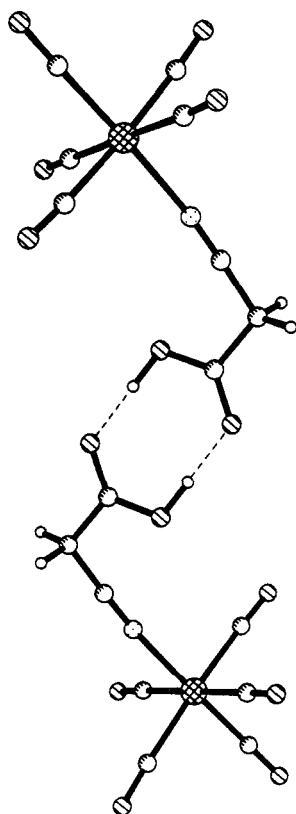


Figure 3. Ball-and-stick representation of **1** indicating intermolecular hydrogen-bonding.

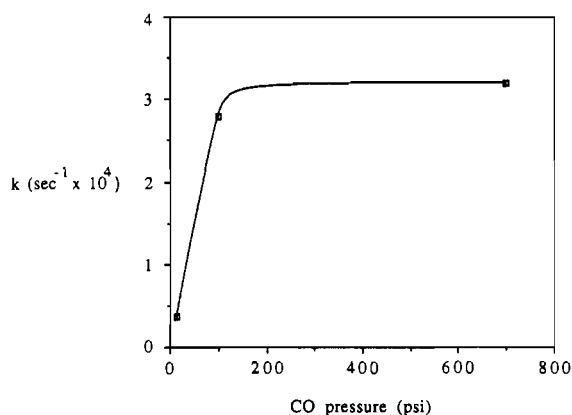


Figure 4. Effect of CO pressure upon rate constant for  $\text{NCCH}_2\text{COOH}$  displacement at 51 °C:  $k = 3.74 \times 10^{-5} \text{ s}^{-1}$  at 14.7 psi,  $2.80 \times 10^{-4} \text{ s}^{-1}$  at 100 psi, and  $3.37 \times 10^{-4} \text{ s}^{-1}$  at 700 psi. For a reaction carried out at 100 psi of CO in the presence of 50 equivalents of  $\text{NCCH}_2\text{COOH}$ ,  $k < 4.0 \times 10^{-6} \text{ s}^{-1}$  at 51 °C.

$\gg$  [NCR]. Reaction 6 was observed to occur at a slower rate under 1 atm of CO pressure than at pressures greater than 200 psi of CO.<sup>11a</sup> No further dependence on CO pressure was noted for reactions studied at higher CO pressures (see Figure 4). Furthermore, reaction 6 was greatly retarded upon addition of 50 equiv (2.55 M) of cyanoacetic acid (see data in Figure 4). The rate data presented in Table VII were obtained at 48.3 atm of CO pressure to avoid any contribution from the reverse reaction.

Figure 5 depicts a selection of the infrared spectra of the  $\nu(\text{CO})$  region measured by the in situ high-pressure infrared technique for a typical kinetic run. Figure 6 illustrates a representative

Table VII. Temperature Dependence of the Rate of Reaction of  $\text{W}(\text{CO})_5(\text{NC-R})$  with CO in THF<sup>a</sup>

temp °C	$10^4 k, \text{ s}^{-1}$		
	$\text{NCCH}_2\text{-COOH}$	$\text{NC}(\text{CH}_2)_{10}\text{-COOH}$	$\text{NCCH}_3$
34.0	0.609	0.248	0.279
45.0	1.91	0.832	1.02
50.0	3.20	1.48	1.78
56.0	5.79	2.65	3.61
60.0	8.15	3.79	4.62

<sup>a</sup> Pressure of CO = 700 psi.

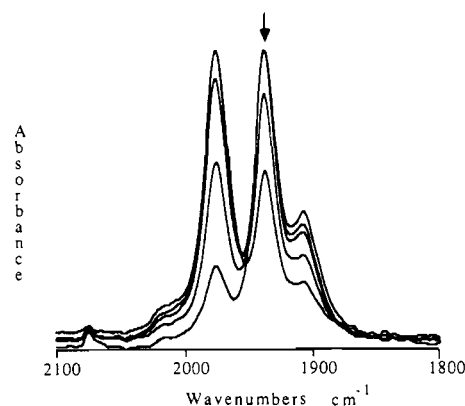


Figure 5. Infrared monitoring of  $\nu(\text{CO})$  region for the reaction of  $\text{W}(\text{CO})_5\text{NC}(\text{CH}_2)_{10}\text{COOH}$  with CO in in situ high-pressure cell (700 psi) at 60 °C.

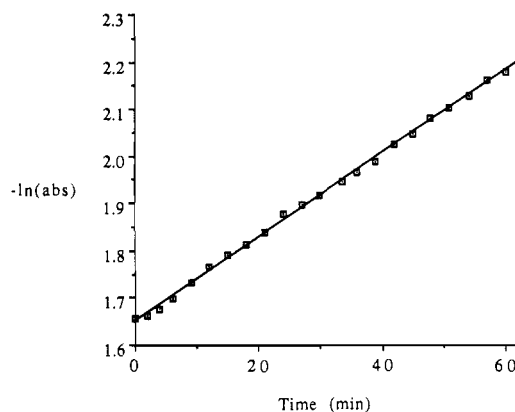


Figure 6. Typical data plot for the ligand substitution reaction of **1** with CO at 700 psi of CO at 40 °C.

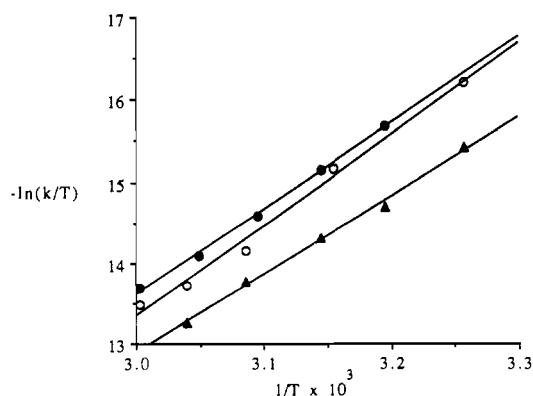


Figure 7. Eyring plots for the ligand substitution reactions of  $\text{W}(\text{CO})_5(\text{NC-R})$  with CO: ( $\blacktriangle$ )  $\text{NCCH}_2\text{COOH}$ ; ( $\bullet$ )  $\text{NC}(\text{CH}_2)_{10}\text{COOH}$ ; ( $\circ$ )  $\text{NCCH}_3$ .

plot of the natural logarithm of the absorbance of the strong E mode  $\nu(\text{CO})$  band as a function of time. Eyring plot for the three nitrile substitution reactions carried out in THF are displayed in Figure 7, whereas the activation parameters may be found in

(11) (a) The solubility of CO in THF is 0.0109 M atm<sup>-1</sup> at 298 K and 0.0117 M atm<sup>-1</sup> at 303 K: Payne, M. W.; Leussing, D. L.; Shore, S. G. *Organometallics* **1991**, *10*, 574. (b) The solubility of CO in *n*-octyl chloride is  $8.21 \times 10^{-3} \text{ M atm}^{-1}$  at 298 K and  $8.71 \times 10^{-3} \text{ M atm}^{-1}$  at 313 K: Calderazzo, F.; Cotton, F. A. *Inorg. Chem.* **1962**, *1*, 30.

**Table VIII.** Activation Parameters  $\Delta H^\ddagger$  and  $\Delta S^\ddagger$  for the Reaction of W(CO)<sub>5</sub>(NC-R) with CO in THF

	NCCH <sub>2</sub> COOH	NC(CH <sub>2</sub> ) <sub>10</sub> COOH	NCCH <sub>3</sub>
$\Delta H^\ddagger$ , kcal mol <sup>-1</sup>	19.4 ± 0.72	20.9 ± 0.51	22.1 ± 1.2
$\Delta S^\ddagger$ , eu	-14.7 ± 2.2	-11.5 ± 1.6	-7.6 ± 3.7

**Table IX.** Temperature Dependence of the Rate of Reaction of W(CO)<sub>5</sub>(NCCH<sub>2</sub>COOH) with CO in CH<sub>2</sub>Cl<sub>2</sub><sup>a</sup>

temp, °C	10 <sup>4</sup> k, s <sup>-1</sup>	$\Delta H^\ddagger$ , kcal/mol	$\Delta S^\ddagger$ , eu
45.0	0.499	29.2 ± 2.3	11.8 ± 7.2
51.0	1.44		
55.0	2.02		
60.0	4.22		

<sup>a</sup> Reactions run at 700 psi of CO.**Table X.** Comparative Inter- and Intramolecular Distances (Å) in the Dimeric Cyanoacetic Acid Unit Bound to Tungsten in **1** and the Free Unit

bond type	bound	free <sup>a</sup>
1	1.15 (1)	1.117 (4)
2	1.47 (1)	1.455 (4)
3	1.512 (9)	1.497 (4)
4	1.217 (7)	1.199 (4)
5	1.311 (9)	1.327 (4)
6	2.627 (3)	2.683 (3)

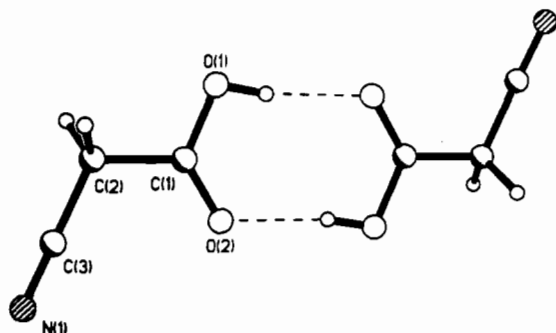
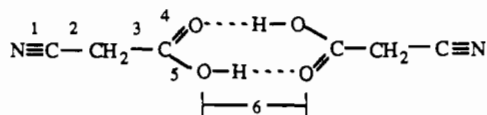
<sup>a</sup> Data taken from ref 12. The  $\beta$  form of cyanoacetic acid is used for comparison. Distances are not significantly different in the  $\alpha$  form.**Figure 8.** Ball-and-stick representation of the atoms connectivity depicting one of the hydrogen-bonding motifs (O-H...O) in free cyanoacetic acid.

Table VIII. The analogous rate data and activation parameters for loss of NCCH<sub>2</sub>COOH from **1** determined in the less-interacting methylene chloride solvent are listed in Table IX.<sup>11b</sup>

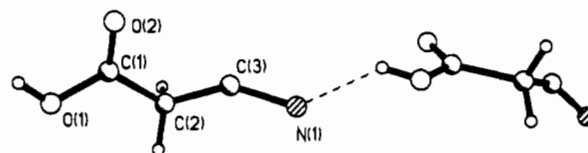
## Discussion

The dimeric structure observed for the cyanoacetic acid derivative of tungsten pentacarbonyl, **1**, is quite similar to what is seen for the cyclic dimer formed by the coupling of two carboxyl groups in the solid-state structure of the free acid.<sup>12,13</sup> A comparison of bond distances for the acid function in complex **1** with the comparable distances in the free acid are provided in Table X. The bond type numbering scheme

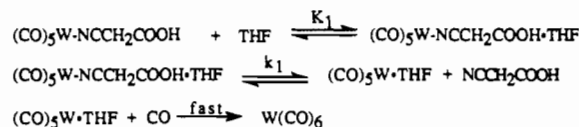


is used in Table X. As is indicated in Table X the intermolecular hydrogen-bonding between two acid units is slightly stronger for the metal complexed acid.

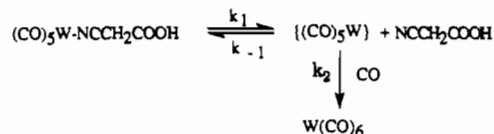
It should however be noted here that the free cyanoacetic acid crystallizes in two distinct crystalline forms, where both forms

**Figure 9.** Ball-and-stick representation of the atoms connectivity depicting one of the hydrogen-bonding motifs (O-H...N) in free cyanoacetic acid.

## Scheme I



## Scheme II



contain two types of hydrogen-bond motifs (see Figures 8 and 9). In the asymmetric unit of the  $\alpha$  form one molecule forms a dimer by carboxyl-group hydrogen bonds while the other two molecules form separate infinite O-H...N-linked polymers. On the other hand the asymmetric unit in the  $\beta$  form contains two independent molecules linked by O-H...N bonding, concomitantly forming a symmetric tetramer by carboxyl-group hydrogen bonding. The O-H...N hydrogen bonding motif is relevant to the catalyzed decarboxylation reaction of cyanoacetic acid by the W(CO)<sub>5</sub>O<sub>2</sub>-CCH<sub>2</sub>CN<sup>-</sup> anion, where an intermediate of the type *cis*-W(CO)<sub>4</sub>(O<sub>2</sub>CCH<sub>2</sub>CN)(NCCH<sub>2</sub>COOH)<sup>-</sup> is proposed.<sup>7</sup> It should be pointed out parenthetically that in the presence of strong base, where the nitrogen-bonded cyanoacetic acid is deprotonated, the cyanoacetate ligand rearranges to the more stable O-bonded isomer, W(CO)<sub>5</sub>O<sub>2</sub>CCH<sub>2</sub>CN<sup>-</sup>. Conversely, addition of 1 equiv of HBF<sub>4</sub> to W(CO)<sub>5</sub>O<sub>2</sub>CCH<sub>2</sub>CN<sup>-</sup> quantitatively affords complex **1**.

The solution structure of **1** in THF has been shown to exist as an equilibrium mixture of complexes containing associated (dimeric) and monomeric carboxyl group, with the latter form being hydrogen-bonded to tetrahydrofuran. Nevertheless, because of the very slight frequency shifts observed in the  $\nu(\text{CO})$  vibrational modes of the {W(CO)<sub>5</sub>} moiety in either of these forms, associated, monomeric/hydrogen-bonded to solvent, or free, it is not expected that this phenomenon has a pronounced effect on the W-N bond dissociation energy.

The kinetic parameters for the displacement of the cyanoacetic acid group in **1** by the poorly nucleophilic carbon monoxide ligand were determined in an effort to measure the W-N binding energy. Unfortunately, in THF solvent these data strongly suggest that the solvent initially displaces the nitrile ligand via an I<sub>d</sub> process, with a subsequent fast process leading to W(CO)<sub>6</sub> (Scheme I).<sup>14</sup> The activation parameters observed for this process ( $\Delta H^\ddagger = 19.4$  kcal mol<sup>-1</sup> and  $\Delta S^\ddagger = -14.7$  eu) are consistent with this reaction pathway. An analogous intimate mechanism accounts for the activation parameters defined for the other nitrile complexes examined in THF solution, i.e., W(CO)<sub>5</sub>NC(CH<sub>2</sub>)<sub>10</sub>COOH and W(CO)<sub>5</sub>NCCH<sub>3</sub>. There appears to be a small increase in bond-breaking character along the series NCCH<sub>2</sub>COOH < NC(CH<sub>2</sub>)<sub>10</sub>COOH < NCCH<sub>3</sub> as reflected in the relative values of the activation parameters (Table VIII).

In Scheme I complex **1** is represented in its monomeric form with no hydrogen-bonding to THF. It is understood that the solution structure of **1** in THF is more complicated (vide supra). However, the W-N bond in all of the various solution species is

(12) Kanters, G. R.; Straver, L. H. *Acta Crystallogr.* **1978**, *B34*, 1393.(13) Kanters, G. R.; Roelofsen, G.; Straver, L. H. *Acta Crystallogr.* **1978**, *B34*, 1396.(14) Darensbourg, D. J. *Adv. Organomet. Chem.* **1982**, *21*, 113.

quite similar. The outer-sphere encounter complex of THF with **1** required for the concerted  $I_d$  process (defined by  $K_1$ ) may not be the same as the hydrogen-bonded carboxylate species. Indeed such an interaction would not be possible for the acetonitrile derivative. Furthermore, it would not be expected to be of importance for the long-chain  $\text{NC}(\text{CH}_2)_{10}\text{COOH}$  acid derivative, since the carboxylic acid function is so remote to the metal center. A possible site for outer-sphere THF interaction common to all three derivatives studied are the acidic CH units adjacent to the  $-\text{CN}$  group.

On the other hand in methylene chloride, a poorly nucleophilic solvent, the reaction proceeds via a dissociative (D) process (Scheme II), with  $\Delta H^\ddagger = 29.2 \text{ kcal mol}^{-1}$  and  $\Delta S^\ddagger = 11.8 \text{ eu}$ . Again it is noteworthy that **1** exists as a mixture of dimer and monomer in methylene chloride (eq 5), but intermolecular hydrogen-bonding has little effect on the W–N bond energy. Although this enthalpy of activation is in accord with corresponding activation parameters determined in other W–L complexes,<sup>15,16</sup> it is significantly lower than the reported W–NCCH<sub>3</sub> bond dissociation energy in  $\text{W}(\text{CO})_5\text{--NCCH}_3$  of 42.7 kcal/mol obtained by calorimetry.<sup>17,18</sup>

### Concluding Remarks

As part of our efforts in exploring metal complexes which may serve as catalysts for the creation of carbon–carbon bonds derived from carbon dioxide, we have focused on reaction 7, the coupling



of carbon dioxide with saturated hydrocarbons to provide carboxylic acids. Reaction 7 is not far from being thermodynamically neutral; i.e., in general the free energy change for this process is only slightly positive. Hence, the barriers for carboxylation and decarboxylation do not differ greatly. Our initial

interest has centered upon examining the mechanistic aspects for the spontaneous reverse process, decarboxylation of the acid.

Relevant to this latter process cyanoacetic acid readily undergoes catalytic and quantitative decarboxylation leading to acetonitrile and carbon dioxide in the presence of  $\text{W}(\text{CO})_5\text{O}_2\text{CCH}_2\text{CN}^-$  (eq 2).<sup>7</sup> In order to define the mechanism for this process it has become apparent that it is necessary to understand the reactions of  $\text{W}(\text{CO})_5\text{O}_2\text{CCH}_2\text{CN}^-$  with excess cyanoacetic acid and subsequently to define the kinetic parameters for loss of the cyanoacetic acid ligand from the metal center. Herein, we have synthesized  $\text{W}(\text{CO})_5\text{NCCH}_2\text{COOH}$  independently from cyanoacetic acid and  $\text{W}(\text{CO})_5\text{THF}$  and characterized its structure both in solution and in the solid state. Furthermore, other studies have verified that the fate of the  $\text{W}(\text{CO})_5\text{O}_2\text{CCH}_2\text{CN}^-$  species upon addition of excess cyanoacetic acid, or 1 equiv of the strong acid  $\text{HBF}_4$ , is formation of the  $\text{W}(\text{CO})_5\text{NCCH}_2\text{COOH}$  complex.<sup>7</sup> Hence the two complexes,  $\text{W}(\text{CO})_5\text{O}_2\text{CCH}_2\text{CN}^-$  and  $\text{W}(\text{CO})_5\text{NCCH}_2\text{COOH}$ , which differ only by a proton, exhibit contrasting reactivity patterns. That is,  $\text{W}(\text{CO})_5\text{O}_2\text{CCH}_2\text{CN}^-$  possesses labile CO ligands and a nonlabile carboxylate group, whereas  $\text{W}(\text{CO})_5\text{NCCH}_2\text{COOH}$  has a labile carboxylic acid ligand and nonlabile CO groups.

Finally, it has been established that the kinetic parameters for displacement of cyanoacetic acid in  $\text{W}(\text{CO})_5\text{NCCH}_2\text{COOH}$  in nucleophilic solvents, such as THF, are indicative of an interchange process ( $I_d$ ). The activation parameters for the interchange process are  $\Delta H^\ddagger = 19.4 \text{ kcal/mol}$  and  $\Delta S^\ddagger = -14.7 \text{ eu}$  or  $\Delta G^\ddagger = 23.8 \text{ kcal/mol}$ . On the other hand, in the less nucleophilic methylene chloride solvent, this ligand substitution process occurs via a dissociative (D) mechanism with  $\Delta H^\ddagger = 29.2 \text{ kcal/mol}$  with  $\Delta S^\ddagger = 11.8 \text{ eu}$  or  $\Delta G^\ddagger = 25.7 \text{ kcal/mol}$ . Both ligand substitution processes presumably occur with the intermediacy of  $\text{W}(\text{CO})_5(\text{solvent})$  complexes.

**Acknowledgment.** The financial support of this research by the National Science Foundation (Grants 88-17873 and 91-19737) is greatly appreciated.

**Supplementary Material Available:** Tables of anisotropic displacement parameters and hydrogen atom coordinates and isotropic displacement parameters for **1** (1 page). Ordering information is given on any current masthead page.

- (15) Yang, G. K.; Peters, K. S.; Vaida, V. *Chem. Phys. Lett.* **1986**, *125*, 566.  
 (16) Bleijereld, R. H. T.; Vrieze, K. *Inorg. Chim. Acta* **1976**, *19*, 195.  
 (17) Adedeji, F. A.; Connor, J. A.; Demain, C. P.; Martino-Simões, J. A.; Skinner, H. A.; Moattar, M. T. Z. *J. Organomet. Chem.* **1978**, *149*, 333.  
 (18) Lewis, K. E.; Golden, D. M.; Smith, G. P. *J. Am. Chem. Soc.* **1984**, *106*, 3905.